Int. J. Solids Structures Vol. 30, No. 13, pp. 1825–1848, 1993
Printed in Great Britain

0020-7683/93 $6.00+.00

ANALYSIS OF COMPOSITE SHEAR WALLS WITH INTERFACE SEPARATION, FRICTION AND SLIP USING BEM

J. T. KATSIKADELIS and F. T. KOKKINOS
Department of Civil Engineering, National Technical University,
Institute of Structural Analysis, Zografou Campus, GR 157 73 Athens, Greece

(*Received* 8 *October* 1991; *in revised form* 16 *December* 1992)

Abstract—In the present investigation a simple, efficient, versatile and easily adaptable, iterative boundary element technique is presented for solving frictional contact problems with tensionless bonding arising in the analysis of composite shear walls and infilled frames. The method is developed using the total deformation formulation and is based on logical steps to establish the contact geometry and regions of slip, interface separation and adhesion. Numerical results are presented to illustrate the method and demonstrate its effectiveness.

1. INTRODUCTION

The study of contact problems between deformable bodies is a modern direction in solid mechanics with important applications in science and technique. These problems which examine the behavior of inclusions embedded in elastic media have several useful applications in civil engineering. The analysis of elastic media which are reinforced with elastic inclusions is of considerable interest to the study of composite materials as well as to the study of composite shear walls and infilled frames.

The contact problems are in general nonlinear and their solution in common formulation is possible only with the help of powerful computer systems and efficient numerical methods, like the Finite Element Method (FEM) and the Boundary Element Method (BEM). The interface between the inclusions and the surrounding elastic medium (matrix material) can exhibit a variety of contact conditions ranging from perfect bonding, frictionless contact with or without separation and frictional contact with or without separation. These problems can be categorized into three types:

(1) Contact without separation and friction, which is a linear and thus reversible problem.
(2) Contact with separation, but without friction, which is a nonlinear but reversible problem.
(3) Contact with separation and friction, which is a nonlinear and irreversible problem. This type of problem is highly nonlinear not only because of the friction phenomenon itself but also because of the changing boundary conditions. The solution to the problem is path dependent and is unique only if the loading history is prescribed.

Thus, when using numerical methods, contact problems have to be solved by iteration and for the frictional case an incremental technique must also be used.

The most popular numerical technique used to perform elastic stress analysis of contacting bodies is the FEM. Fredriksson (1976) employed the concept of a contact stress increment vector and a slip increment vector at a contact surface, with a general slip criterion to solve the incremental governing equations by means of a finite displacement method. Okamoto and Nakazawa (1979) used a load incrementation theory with various frictional conditions. Torstenfelt (1983, 1984) solved contact problems with friction using automatic incrementation techniques in general-purpose FE computer programs. Heyliger and Reddy (1987) introduced a mixed computational algorithm and corresponding finite element model for the analysis of plane elastic contact problems assuming large deformations and approximating the nodal displacements and stresses independently. Sachdeva and Ramakrishnan (1981) developed a total deformation formulation procedure to deal with

two-dimensional elastic contact problems with friction. Achyutha *et al.* (1986) presented a simple iterative FE method to study the behavior of infilled frames with openings, taking into consideration separation, slip and frictional loss at the interface of the infill and the wall.

The BEM is particularly well suited for contact problems since only the boundaries which are of primary interest in the solution procedure are treated and hence the interior of the model does not need to be discretized as with finite differences or finite elements. Hence the time required to model a problem using boundary elements is much shorter than, for instance, for finite elements. Also, the boundary displacement and traction vector unknowns are calculated with the same degree of accuracy and the normal and tangential tractions can be coupled directly in the equation system. These are important features, especially for problems such as contact. Andersson *et al.* (1980) applied the boundary integral equation method to two-dimensional frictionless problems using constant elements with successful results, and later extended the applications to frictional contact (Andersson, 1981). Andersson also treated the problem using linear parabolic elements (Andersson, 1982). In his approach, he uses the final deformed configuration as the state of reference and assumes a point contact or a contact of finite length between the two bodies. This analysis is based on the assumption of a single and open initial contact zone between two bodies and is not easily and efficiently applied to the case of multiple contact zones between several bodies, where there are coupled effects between the different contact areas. Moreover, for the case of frictional contact Andersson employs an incremental procedure and establishes a new area of contact at each load increment on the basis of a scaling procedure, which requires a lot of computer time, and inevitably restricts the analysis to a small system of equations. Selvadurai and Ap (1985) studied the effects of inclusions embedded in an elastic medium of finite extent. Paris and Garrido (1985) used discontinuous elements to solve typical two-dimensional friction contact problems. They also used an incremental procedure to study the case of friction contact problems where more than one contact zone and more than one chapter of load are involved (Paris and Garrido, 1988). Garrido *et al.* (1989) dealt with three-dimensional contact problems, assuming an elastic behavior in the contacting bodies and confining the analysis to frictionless surfaces and initially conforming contact. Gakwaya and Lambert (1989) presented a numerical algorithm for the solution of a three-dimensional quasi-static contact problem with friction using a boundary element and mathematical programming approach. Takahashi and Brebbia (1988) analysed contact problems with and without friction using discontinuous constant elements and substructuring techniques, and Jin *et al.* (1987) employed an incremental friction theory based on the nonlocal and nonlinear friction law aimed at a more fundamental modeling of the microscopic mechanism of the friction phenomenon.

In the present investigation a simple, efficient, versatile, easily adaptable and computationally fast, iterative boundary element technique is described for solving frictional contact problems with tensionless bonding arising in the analysis of composite shear walls and infilled frames. The method is developed using the total deformation formulation and is based on logical steps to accurately predict the contact geometry and regions of slip, interface separation and adhesion. The proposed approach uses the initial undeformed configuration as a state of reference where the matrix and inclusions are assumed to be completely bonded along the interfaces. It accounts for complicated geometries, arbitrary loading, any type of boundary conditions and multiple inclusions. This algorithm is applicable to proportional loading cases only. However, the method can easily be generalized for nonproportional loading cases by giving small load increments and using an iterative procedure for convergence in each incremental step. It is simple in nature and needs very few iterations for convergence. Several test and practical examples are presented showing the validity, versatility and effectiveness of the method.

2. FORMULATION OF THE PROBLEM

Consider a shear wall of arbitrary shape (Fig. 1) consisting of a matrix material occupying a two-dimensional region R_1 in the x_1x_2 plane with modulus of elasticity, E_1,

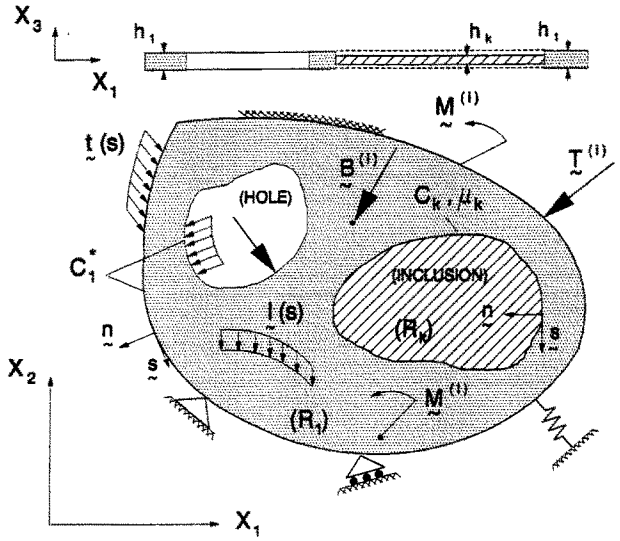

Fig. 1. Geometry, loading and support conditions of a composite shear wall.

and Poisson's ratio, ν_1, and surrounding a finite number of inclusions (infill walls) occupying the regions R_k with elastic constants, E_k and ν_k $(k = 2, 3, \ldots, K)$, and a Coulomb frictional coefficient, μ_k, between the two surfaces in contact. The material of the matrix and inclusions is assumed to be homogeneous, isotropic and linearly elastic. The constant thickness h_1 of the matrix material and h_k of the kth inclusion are small compared with the other dimensions so that the assumptions of the plane stress problem are satisfied. Let the boundaries of the regions R_k be denoted by C_k $(k = 2, 3, \ldots, K)$ and the external boundary by C_1^*, as shown in Fig. 1; then the boundary C_1 of the matrix will be $C_1 = C_1^* \cup C_2 \cup C_3 \cup \ldots \cup C_K$. The boundary curves C_k $(k = 1, 2, \ldots, K)$ are piecewise smooth, that is they may have a finite number of corners. If any of the regions R_k are holes the problem can be solved by treating its boundary as an exterior one.

The loading of the wall is applied symmetrically with respect to its middle plane and consists of:

(a) Loads acting on the boundary: distributed traction $\mathbf{t}(s)$, concentrated forces $\mathbf{T}^{(i)}$ $(i = 1, 2, \ldots, n_1)$ and concentrated moments $\mathbf{M}^{(i)}$ $(i = 1, 2, \ldots, n_2)$.

(b) Loads acting inside $R^* = \bigcup_{k=1}^{K} R_k$ (body forces): distributed body forces $\mathbf{b}(x)$, line loads $\mathbf{l}(s)$ distributed along a curve L, concentrated forces $\mathbf{B}^{(i)}$ $(i = 1, 2, \ldots, n_3)$ and concentrated moments $\mathbf{M}^{(i)}$ $(i = 1, 2, \ldots, n_4)$.

Regarding the support conditions of the wall its boundary may be

(a) Free (second boundary value problem).
(b) Clamped or subjected to prescribed displacements along the entire boundary (first boundary value problem), along parts of it and or at discrete points (mixed boundary value problem).
(c) Elastically supported along a part or at discrete points of the boundary.
(d) Simply supported in a prescribed direction at a point.

With the assumption that the thickness of the shear wall is small compared to its other two dimensions the resulting state of stress is two-dimensional, thus, the stress, the strain, and the displacement components depend only on the x_1, x_2 coordinates (plane stress problem). In this case, the governing equations of the problem in terms of the displacements in each region R_k $(k = 1, 2, \ldots, K)$ are the Navier equations of equilibrium:

$$\nabla^2 u_i + \frac{1}{1-2\bar{\nu}_k} \frac{\partial}{\partial x_i}\left(\frac{\partial u_j}{\partial x_j}\right) + \frac{1}{G_k} b_i = 0, \quad (i, j = 1, 2), \tag{1}$$

where G_k is the shear modulus and $\bar{\nu}_k = 1/(1+\nu_k)$ is the effective Poisson's ratio of the kth material; $\nabla^2 = \partial^2/\partial x_1^2 + \partial^2/\partial x_2^2$ is the two-dimensional Laplace operator.

We denote by C_u the part of the boundary on which the displacements are prescribed and by C_t its complementary part on which the tractions are prescribed (it is $C_u \cup C_t = C$, $C_u \cap C_t = \{\varnothing\}$) then the following boundary conditions must be satisfied:

$$u_i = u_i(s) \quad \text{on} \quad C_u, \tag{2a}$$

$$t_i = t_i(s) \quad \text{on} \quad C_t, \tag{2b}$$

where $u_i(s)$ and $t_i(s)$ are prescribed functions of the arc length along the boundary.

When a part C_e of the boundary is elastically supported the following boundary conditions must be satisfied:

$$\alpha_1(s)u_n + \beta_1(s)t_n = \gamma_1(s), \tag{3a}$$

$$\alpha_2(s)u_s + \beta_2(s)t_s = \gamma_2(s), \tag{3b}$$

in which $\alpha_i(s)$, $\beta_i(s)$ and $\gamma_i(s)$ $(i = 1, 2)$ are given functions defined on the boundary; and u_n, t_n, u_s, t_s are the displacement and traction components on the boundary in the normal and tangential directions. Notice that the boundary conditions (3a), (3b) are the most general case of linear boundary conditions, from which all other boundary conditions can be derived by specifying appropriately the functions $\alpha_i(s)$, $\beta_i(s)$ and $\gamma_i(s)$.

Furthermore, additional boundary conditions (contact conditions) must be satisfied on the interfaces C_k $(k = 2, 3, \ldots, K)$ between matrix and inclusions. These boundary conditions are established from the following physical considerations which are based on the type of contact between the two elastic bodies:

(i) *Perfect bonding*

The traction components are equal in magnitude and opposite in direction, while the displacement components remain continuous across the interface. These conditions can be expressed in equation form as:

$$u_i^{(1)} = u_i^{(k)}, \tag{4a}$$

$$t_i^{(1)} + t_i^{(k)} = 0, \quad (i = 1, 2). \tag{4b}$$

(ii) *Bilateral contact with slipping*

The traction components are equal in magnitude and opposite in direction. Moreover, the traction components in the tangential direction satisfy the Coulomb frictional law and the displacement components in the normal direction are equal in order to preserve the continuity in this direction. These conditions are written as:

$$u_n^{(1)} = u_n^{(k)}, \tag{5a}$$

$$t_i^{(1)} + t_i^{(k)} = 0, \quad (i = 1, 2), \tag{5b}$$

$$t_s^{(1)} = \pm \mu t_n^{(1)}, \tag{5c}$$

where the subscripts n and s denote the normal and tangential directions (Fig. 1), respectively, μ is the friction coefficient and the sign in the third condition is chosen to oppose the relative motion at the surface. The case $\mu = 0$ refers to a frictionless contact.

(iii) *Interface separation*

In this case the displacement continuity is lost along a part of the interface and the separated boundaries are free of tractions. The interface conditions are written as:

$$t_i^{(1)} = 0, \tag{6a}$$

$$t_i^{(k)} = 0, \quad (i = 1, 2). \tag{6b}$$

The integral representation of the solution for the points on the boundary C_k $(k = 1, 2, \ldots, K)$ is given by the following integral representation (Katsikadelis and Kokkinos, 1987):

$$\tfrac{1}{2}u_j^{(k)}(\mathbf{x}) = \int_{C_k} [t_i^{(k)}(\boldsymbol{\xi}) U_{ij}^{(k)}(\boldsymbol{\xi}, \mathbf{x}) - u_i^{(k)}(\boldsymbol{\xi}) T_{ij}^{(k)}(\boldsymbol{\xi}, \mathbf{x})]\, \mathrm{d}s_\xi + \int_{R_k}\int b_i^{(k)}(\mathbf{Z}) U_{ij}^{(k)}(\mathbf{Z}, \mathbf{x})\, \mathrm{d}\sigma_z, \quad (i, j = 1, 2), \tag{7}$$

where $\mathbf{x}, \boldsymbol{\xi} \in C_k$ and $\mathbf{Z} \in R_k$. The indices of the elements $\mathrm{d}s$ and $\mathrm{d}\sigma$ denote the point which varies during integration. $U_{ij}(\boldsymbol{\xi}, \mathbf{x})$ and $T_{ij}(\boldsymbol{\xi}, \mathbf{x})$ are two-point tensors denoting displacement and traction, respectively, at point $\mathbf{x}$ in the direction of the x_i axis due to a unit concentrated force at point $\boldsymbol{\xi}$ in the direction of the x_j axis (Katsikadelis and Kokkinos, 1987).

Equation (7) relates the displacements u_i to the tractions t_i on the boundary C_k. They are integral equations which may be solved together with the boundary conditions (2a, b) or (3a, b) and the contact conditions (4a, b), (5a–c) and (6a, b) to establish the unknown boundary displacements u_i and tractions t_i. Subsequently, the displacements inside the region R_k are given as (Katsikadelis and Kokkinos, 1987):

$$u_j^{(k)}(\mathbf{X}) = \int_{C_k} [t_i^{(k)}(\boldsymbol{\xi}) U_{ij}^{(k)}(\boldsymbol{\xi}, \mathbf{X}) - u_i^{(k)}(\boldsymbol{\xi}) T_{ij}^{(k)}(\boldsymbol{\xi}, \mathbf{X})]\, \mathrm{d}s_\xi + \int_{R_k}\int b_i^{(k)}(\mathbf{Z}) U_{ij}^{(k)}(\mathbf{Z}, \mathbf{X})\, \mathrm{d}\sigma_z, \quad (i, j = 1, 2), \tag{8}$$

where $\mathbf{X}(x_1, x_2)$ and $\mathbf{Z}(z_1, z_2)$ are points inside the region R_k while $\boldsymbol{\xi}(\xi_1, \xi_2)$ are points on its boundary, C_k.

3. NUMERICAL IMPLEMENTATION

The boundary integral representation of the solution and its numerical treatment is obtained using the boundary element approach presented by Katsikadelis and Kokkinos (1987). In this investigation the boundaries $C_1^*, C_2, \ldots, C_K$ are divided into $N_1^*, N_2, \ldots, N_K$ boundary elements, respectively. The elements are not necessarily equal. The elements on the external boundary are numbered consecutively counterclockwise while on the internal boundaries they are numbered clockwise (Fig. 2). The values of the unknown boundary functions $u_i^{(k)}$ and $t_i^{(k)}$ $(i = 1, 2; k = 1, 2, \ldots, K)$ are assumed constant on each element (step function assumption) and equal to their values at the nodal point of each element. Moreover, the boundary element is approximated by a parabolic arc (Katsikadelis and Sapountzakis, 1985).

Denoting by $[u]_m$ and $[t]_m$ the displacement and traction components at the nodal point m, of the discretized boundary, eqn (7) is written as:

$$\tfrac{1}{2}[u]_m^{(1)} = \sum_{l=1}^{N} [G]_{ml}^{(1)}[t]_l^{(1)} - \sum_{l=1}^{N} [H]_{ml}^{(1)}[u]_l^{(1)} + [F]_m^{(1)}, \tag{9a}$$

$$\tfrac{1}{2}[u]_m^{(k)} = \sum_{l=S_{k-1}+1}^{S_k} [G]_{ml}^{(k)}[t]_l^{(k)} - \sum_{l=S_{k-1}+1}^{S_k} [H]_{ml}^{(k)}[u]_l^{(k)} + [F]_m^{(k)}, \quad (m = S_{k-1}+1, S_{k-1}+2, \ldots, S_k;\ k = 2, 3, \ldots, K), \tag{9b}$$

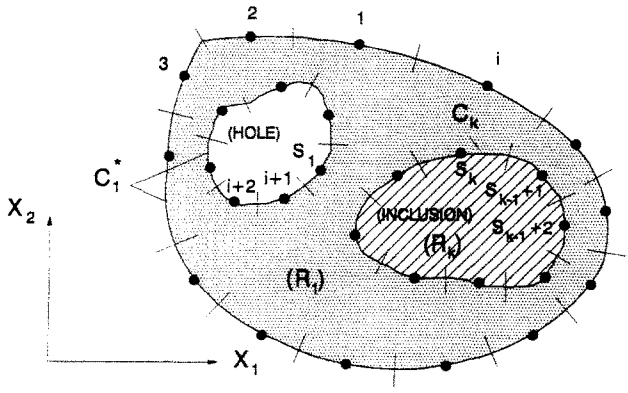

Fig. 2. Typical discretization of the boundaries of a composite shear wall.

in which $S_1 = N_1^*$, $S_2 = S_1 + N_2, \ldots, S_k = S_{k-1} + N_k$ and $S_K = N, N =$ total number of elements, and

$$[G]_{ml}^{(k)} = \begin{bmatrix} \int_l U_{11}^{(k)}(\xi, \mathbf{x})\, ds_\xi & \int_l U_{21}^{(k)}(\xi, \mathbf{x})\, ds_\xi \\ \int_l U_{12}^{(k)}(\xi, \mathbf{x})\, ds_\xi & \int_l U_{22}^{(k)}(\xi, \mathbf{x})\, ds_\xi \end{bmatrix}, \tag{10a}$$

$$[H]_{ml}^{(k)} = \begin{bmatrix} \int_l T_{11}^{(k)}(\xi, \mathbf{x})\, ds_\xi & \int_l T_{21}^{(k)}(\xi, \mathbf{x})\, ds_\xi \\ \int_l T_{12}^{(k)}(\xi, \mathbf{x})\, ds_\xi & \int_l T_{22}^{(k)}(\xi, \mathbf{x})\, ds_\xi \end{bmatrix}, \tag{10b}$$

$$[F]_m^{(k)} = \begin{bmatrix} \int_{R_k} \int [U_{11}^{(k)}(\mathbf{Z}, \mathbf{x})\, b_1^{(k)}(\mathbf{Z}) + U_{21}^{(k)}(\mathbf{Z}, \mathbf{x})\, b_2^{(k)}(\mathbf{Z})]\, d\sigma_z \\ \int_{R_k} \int [U_{12}^{(k)}(\mathbf{Z}, \mathbf{x})\, b_1^{(k)}(\mathbf{Z}) + U_{22}^{(k)}(\mathbf{Z}, \mathbf{x})\, b_2^{(k)}(\mathbf{Z})]\, d\sigma_z \end{bmatrix}, \tag{10c}$$

$\xi \in l$-element, $\mathbf{x}$ the m-nodal point and $\mathbf{Z} \in R_k$.

Equations (9a, b) constitute a system of $2N + 2(N - N_1^*)$ simultaneous linear algebraic equations in $4N + 4(N - N_1^*)$ unknowns. The additional $4(N - N_1^*) + 2N_1^*$ which are required to establish the unknown quantities are derived from the boundary conditions (3a, b), (4a, b), (5a–c) and (6a, b). More specifically, eqns (3a, b) applied to all nodal points of the external boundary C_1^*, yield the following $2N_1^*$ algebraic equations:

$$[\alpha]_m [u]_m^{(1)} + [\beta]_m [t]_m^{(1)} = [\gamma]_m, \tag{11}$$

where the matrices $[\alpha]_m$, $[\beta]_m$ with dimensions 2×2 and the matrix $[\gamma]_m$ with dimensions 2×1, are given as:

$$[\alpha]_m = \begin{bmatrix} \alpha_1^{(m)} \cos\theta_m & \alpha_1^{(m)} \sin\theta_m \\ -\alpha_2^{(m)} \sin\theta_m & \alpha_2^{(m)} \cos\theta_m \end{bmatrix},$$

$$[\beta]_m = \begin{bmatrix} \beta_1^{(m)} \cos\theta_m & \beta_1^{(m)} \sin\theta_m \\ -\beta_2^{(m)} \sin\theta_m & \beta_2^{(m)} \cos\theta_m \end{bmatrix}, \quad [\gamma]_m = \begin{bmatrix} \gamma_1^{(m)} \\ \gamma_2^{(m)} \end{bmatrix}, \tag{12}$$

in which $\alpha_i^{(m)}$, $\beta_i^{(m)}$, $\gamma_i^{(m)}$ $(i = 1, 2;\ m = 1, 2, \ldots, N_1^*)$ are the values of the functions $\alpha_i(s)$,

$\beta_i(s)$, $\gamma_i(s)$ at the nodal point m, and θ_m is the angle between the x_1 axis and the outward normal vector n_m to the boundary C_1^* at the nodal point m.

The remaining $4(N-N_1^*)$ equations are obtained from the contact conditions applied at the interface between the inclusions and the matrix material [eqns (4a, b), (5a–c) and (6a, b)]. These equations are written in general form as:

$$[a]_m[u]_m^{(1)} + [b]_m[u]_m^{(k)} = [0], \tag{13a}$$

$$[c]_m[t]_m^{(1)} + [d]_m[t]_m^{(k)} = [0], \tag{13b}$$

$$(m = S_{k-1}+1, S_{k-1}+2, \ldots, S_k\,;\, k = 2, 3, \ldots, K),$$

where the matrices $[a]_m$, [b]$_m$, $[c]_m$ and $[d]_m$ with dimensions 2×2, are defined according to the type of contact at the m-element of the matrix – k th inclusion interface.

In practice the area of contact is not known *a priori* since some of the nodal points lose contact, others may slip, while the rest may be bonded. The separation, slip and frictional loss at the interface of the matrix and inclusions are allowed by the following iterative procedure:

(1) The analysis is made with full contact at the interface.
(2) An algorithm is used to test the contact conditions and to determine if any changes are required, according to the following steps:
   (i) The normal tractions along the interface must be negative, otherwise the nodal point is deleted from the possible contact zone and is inserted in the free zone.
   (ii) If the ratio of a nodal traction in the tangential direction to the corresponding nodal traction in the normal direction is greater than the friction coefficient, slipping occurs.
   (iii) If a node is in the contact zone and slipping is permitted, the tangential traction and displacement must be in opposite directions. Otherwise the node will be included in the adhesion zone for the next iteration.
   (iv) Nodes on the free inclusion boundaries must not penetrate into the region of the deformed matrix (material overlap). If this occurs then these nodes must be reincorporated in the adhesion zone. It is worth noting that in this investigation the penetration test is realized by examining the relative position of the nodal points of the inclusion with respect to the deformed configuration of the matrix boundary. Since the deformed boundary is described by the displaced position of the nodal points, its deformed configuration is locally approximated by a parabolic arc passing through the nodal point of consideration and its two adjacent nodal points (Fig. 3).
(3) If during the second step there are no incompatibilities observed, then the procedure has converged and a stable configuration has been obtained.
(4) All the changes detected in the second step are introduced into the boundary conditions and the problem is solved again.

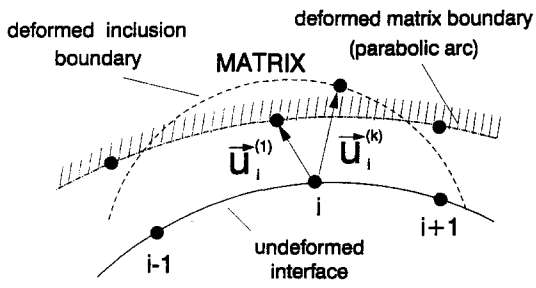

Fig. 3. Free inclusion node penetrating into the region of the deformed matrix (material overlap).

Steps 2–4 are repeated until no separation, slip or displacement incompatibility occur. Once the regions of contact and separation have been determined, the boundary quantities of the problem will be known and then the displacement and stress components in the interior of the elastic bodies are evaluated using the formulation presented by Katsikadelis and Kokkinos (1987).

4. NUMERICAL RESULTS

On the basis of the analysis and the numerical procedure presented in the previous sections, a computer program has been written and numerical results have been obtained for composite shear walls with a variety of shapes subjected to several types of loading. A special emphasis is laid on the analysis of the complicated problem of infilled frames in order to determine the effect of the wall characteristics and contact conditions at the interface, on the overall stiffness of frame structures.

The first problem treated is a rectangular cantilever wall with a rectangular inclusion (Fig. 4). The matrix material is characterized by modulus of elasticity $E_m = 10^6$ N cm^{-2},

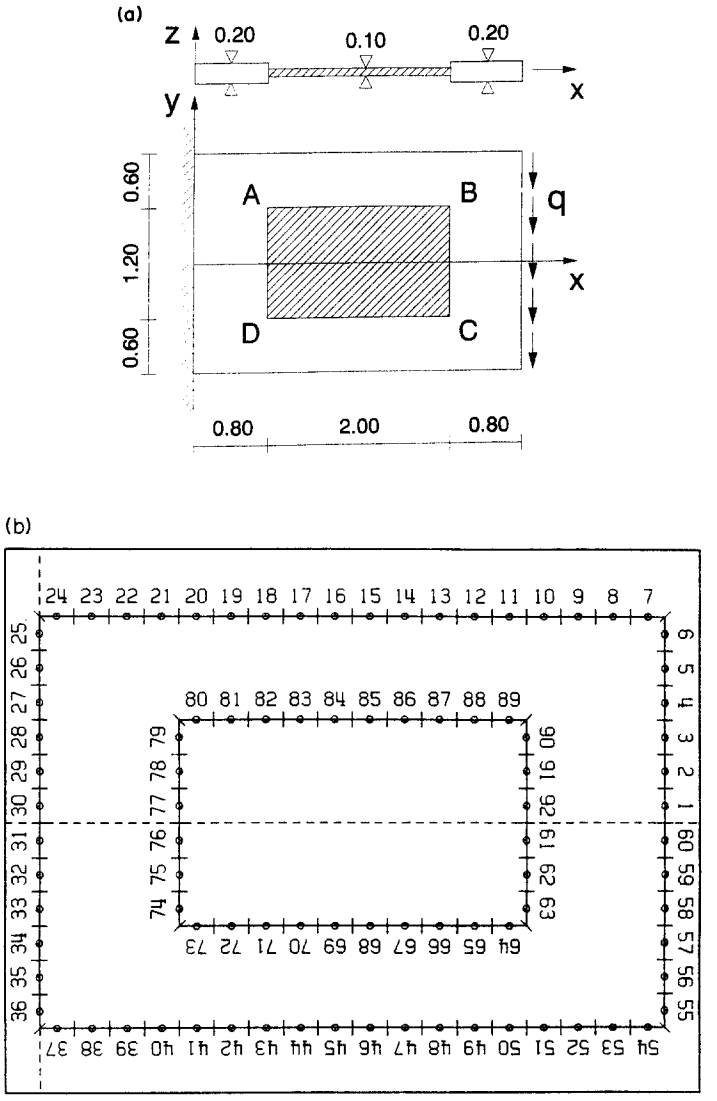

Fig. 4. Loading, support conditions and discretization of rectangular cantilever wall with rectangular inclusion. (a) Loading and support conditions. (b) Discretization of the boundaries (92 constant elements).

Poisson's ratio $\nu_m = 0.30$ and has thickness $h_m = 20$ cm, while for the inclusion the corresponding values are $E_i = 2 \times 10^5$ N cm^{-2}, $\nu_i = 0.15$ and $h_i = 10$ cm. The composite wall is clamped at one end ($u_x(x, y) = u_y(x, y) = 0$ at $x = 0$) and subjected to a uniform shear load $q = 500$ N cm^{-2} at the free end. The wall is analysed first assuming perfect bond along the interface $ABCD$ of the matrix and inclusion and then assuming tensionless contact ($\mu = \infty$). The deformed configuration and the flow of principal stresses are given for both cases in Figs 5 and 6, respectively. The distribution of the normal and shear matrix tractions developed along the interface $ABCD$ are given in Fig. 7 for the case of complete bond, and in Fig. 8 for the case of tensionless bonding.

The second example is a plane strain problem. A very long structure having the composite trapezoid cross-section of Fig. 9(a), is loaded with two uniform vertical loads of magnitudes $p_1 = 250$ kN m^{-2} and $p_2 = 2250$ kN m^{-2}, which remain constant along its

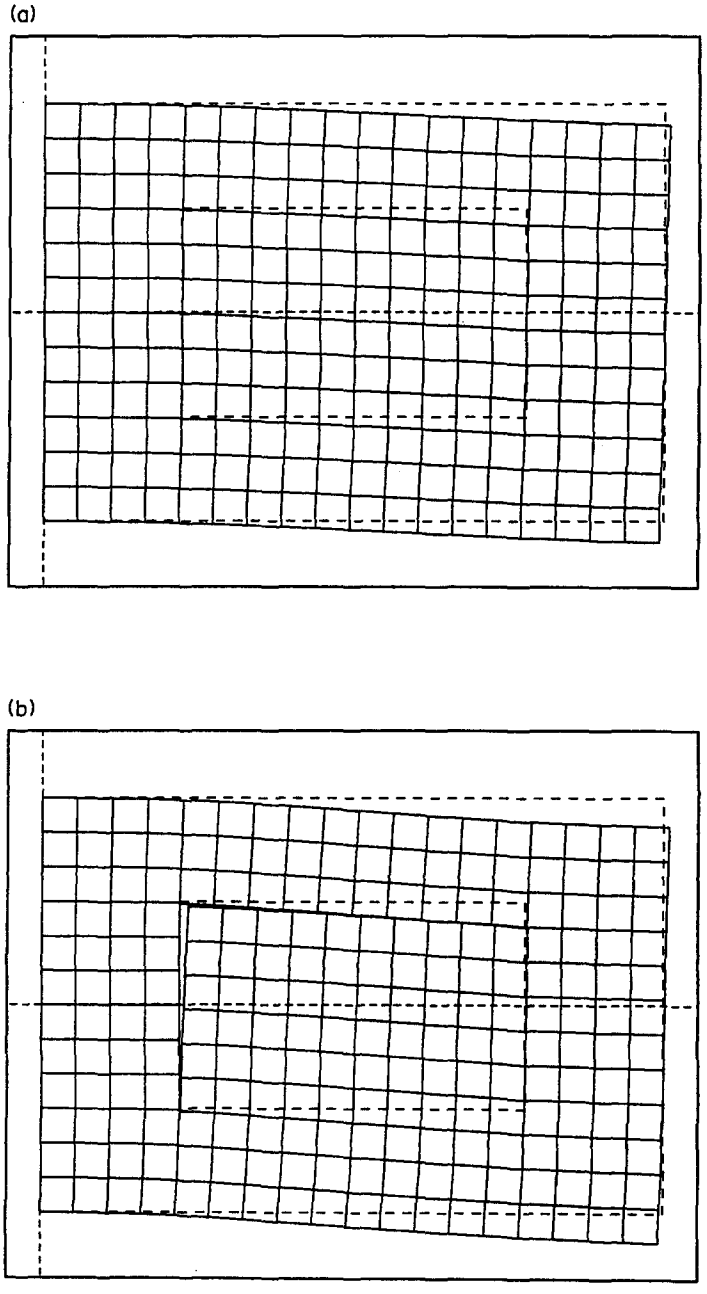

Fig. 5. Deformed shape of the composite cantilever wall. (a) Perfect bond. (b) Tensionless contact ($\mu = \infty$).

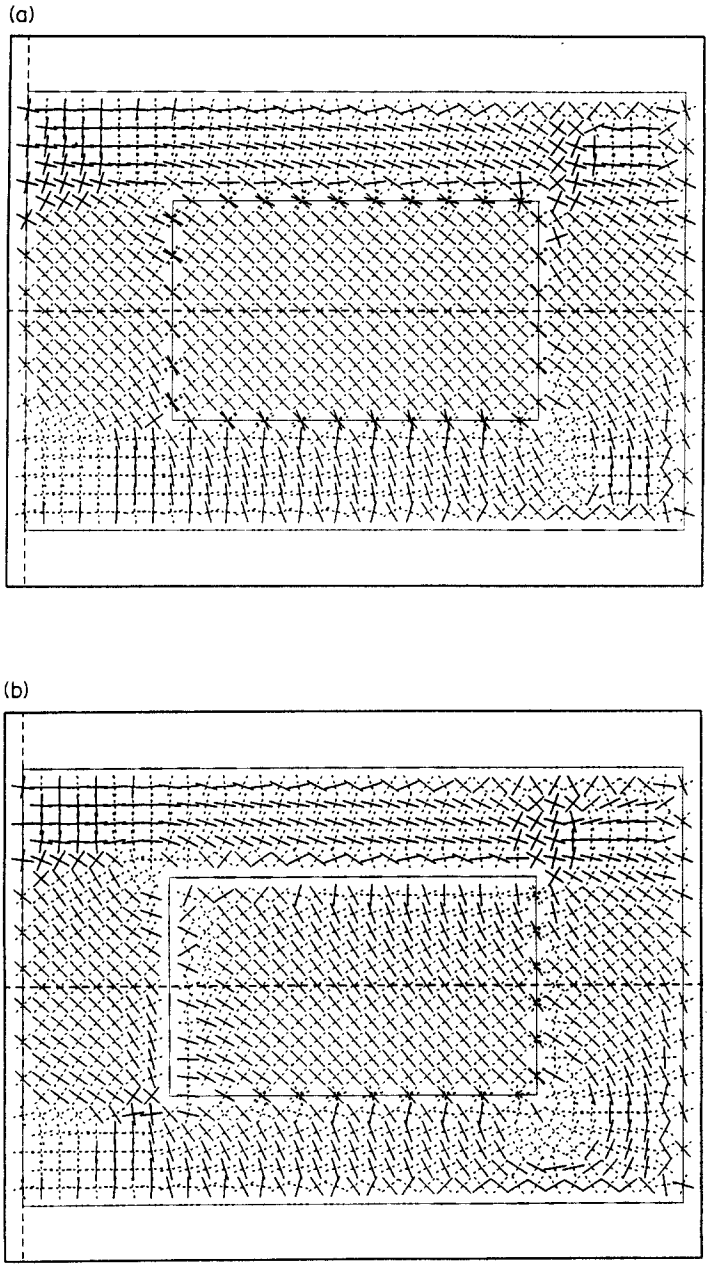

Fig. 6. Flow of principal stresses of the composite cantilever wall. (a) Perfect bond. (b) Tensionless contact ($\mu = \infty$).

length. The displacement pattern of a typical composite section ($E_m = 2 \times 10^6$ kN m^{-2}, $E_i = 0.05E_m$, $\nu_m = 0.30$, $\nu_i = 0.15$) is presented for two types of contact: perfect bond and frictional slip with $\mu = 1.75$ in Figs. 10(a) and 10(b). A more complicated plane strain problem is given in Fig. 11. The elastic constants of the matrix are $E_m = 10^6$ kN m^{-2}, $\nu_m = 0.25$, of the first inclusion $E_i^{(1)} = 0.05E_m$, $\nu_i^{(1)} = 0.15$ and of the second $E_i^{(2)} = 0.20E_m$, $\nu_i^{(2)} = 0.20$. The friction coefficient is the same along both interfaces, $\mu = 0.75$. The composite structure is subjected to a uniformly distributed vertical load $p = 800$ kN m^{-2} at the top and a uniform shear load $q = 8000$ kN m^{-2} at the side (see Fig. 11). In Fig. 12, the deformed configuration for the case of perfect bond between the different materials is compared to the one obtained assuming frictional contact with $\mu = 0.75$. The distribution of the normal and shear stresses developed on the matrix along the two interfaces is given in Figs 13 and 14, for both cases of contact conditions.

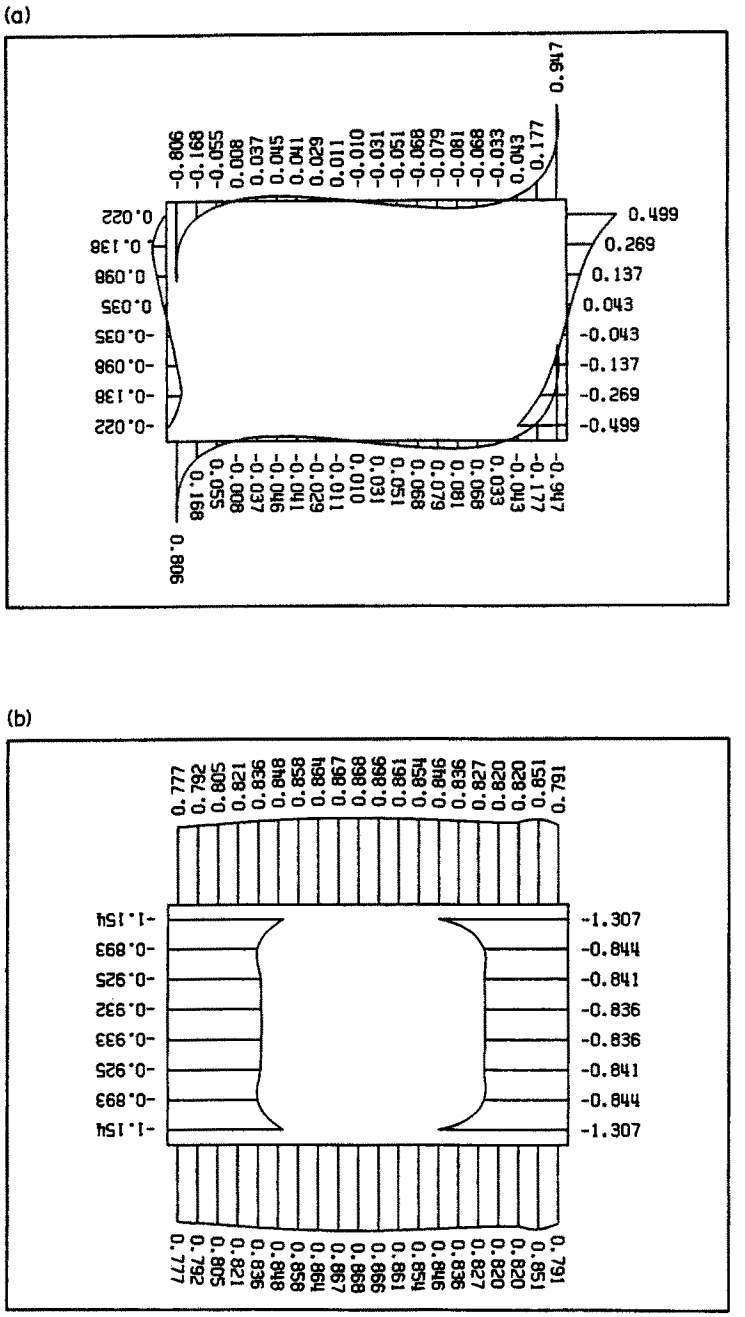

Fig. 7. Distribution of normalized stresses (σ_{ij}/q) along the matrix-inclusion interface of the cantilever wall for the case of perfect bond. (a) Normal stresses. (b) Shear stresses.

Finally, an infilled frame is analysed in order to determine the effect of the geometry, material characteristics and contact conditions at the interface, on the overall stiffness of the structure. The concrete frame (matrix material) is clamped in the rectangular foundation *BCDE*, which is firmly bonded to the elastic half space. The frame has modulus of elasticity $E_f = 2.1 \times 10^7$ kN m^{-2}, Poisson's ratio $\nu_f = 0.20$ and is subjected to shear loads $p = 3 \times 10^3$ kN m^{-2} at the top of its columns [Fig. 15(a)]. The infill of width b and height h, is characterized by elastic constants E_w and $\nu_w = 0.075$. Both the frame and the infill wall have thickness $t = 0.25$ m. Figures 15(a), 15(b) and 15(c) give the deformed configuration of the frame without infill wall, with an infill wall perfectly bonded to the frame ($E_w/E_f = 0.20$), and with an infill wall being in frictional contact with the frame ($E_w/E_f = 0.20$, $\mu = 0.60$), respectively. Figure 16(a) depicts the lateral stiffness of the two-column frame ($K = P/u_A$,

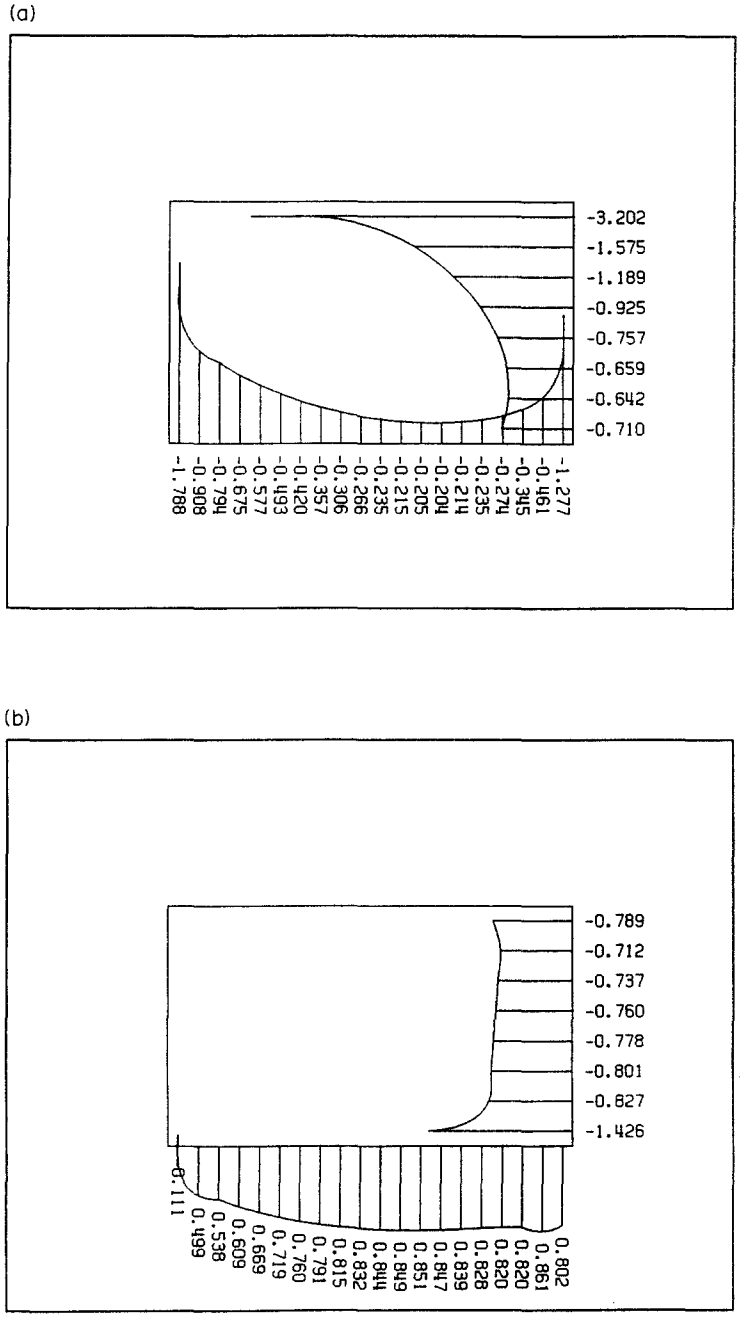

Fig. 8. Distribution of stresses (normalized, σ_{ij}/q) along the matrix-inclusion interface of the cantilever wall for the case of tensionless contact ($\mu = \infty$). (a) Normal stresses. (b) Shear stresses.

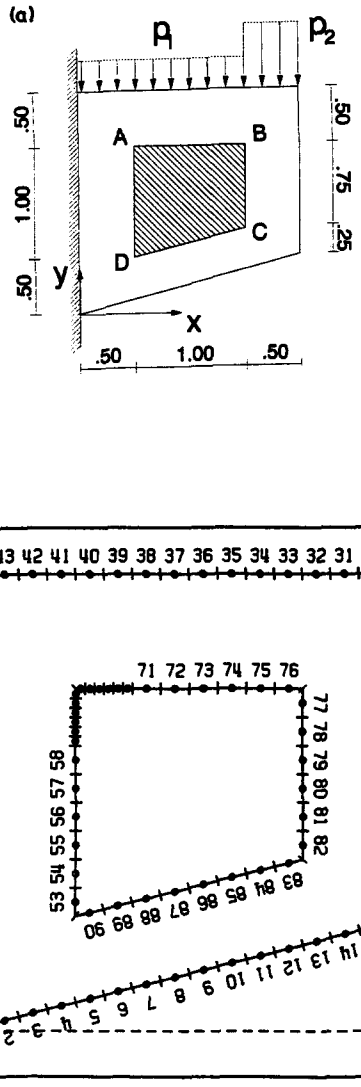

Fig. 9. Geometry, loading, support conditions and discretization of composite cross-section. (a) Geometry and loading. (b) Discretization of the boundaries (90 constant elements).

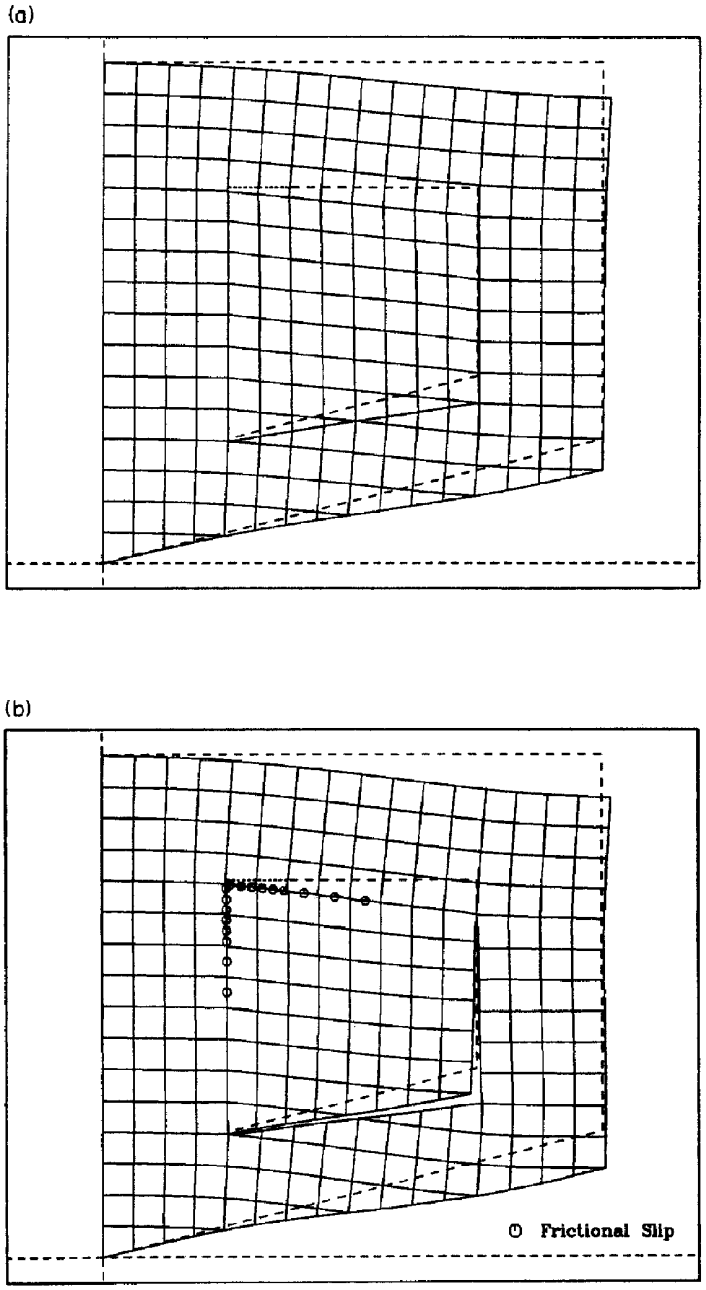

Fig. 10. Deformation pattern of composite cross-section for different contact conditions. (a) Perfect bond. (b) Frictional slip ($\mu = 1.75$).

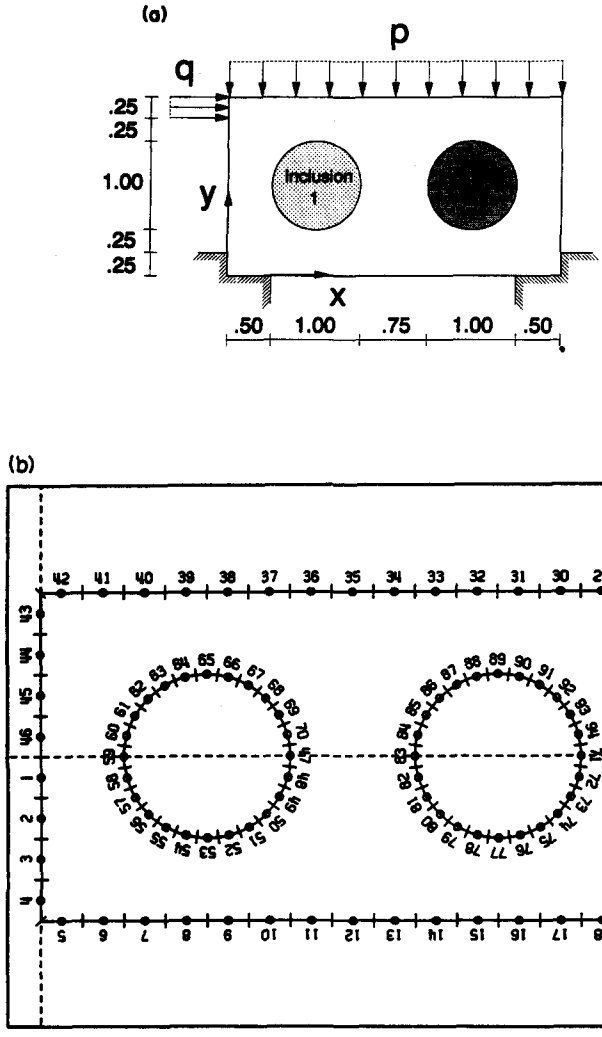

Fig. 11. Composite rectangular cross-section with circular inclusions ($E_1^{(1)} = 0.05E_m$, $E_1^{(2)} = 0.20E_m$). (a) Geometry and loading. (b) Discretization of the boundaries (94 constant elements).

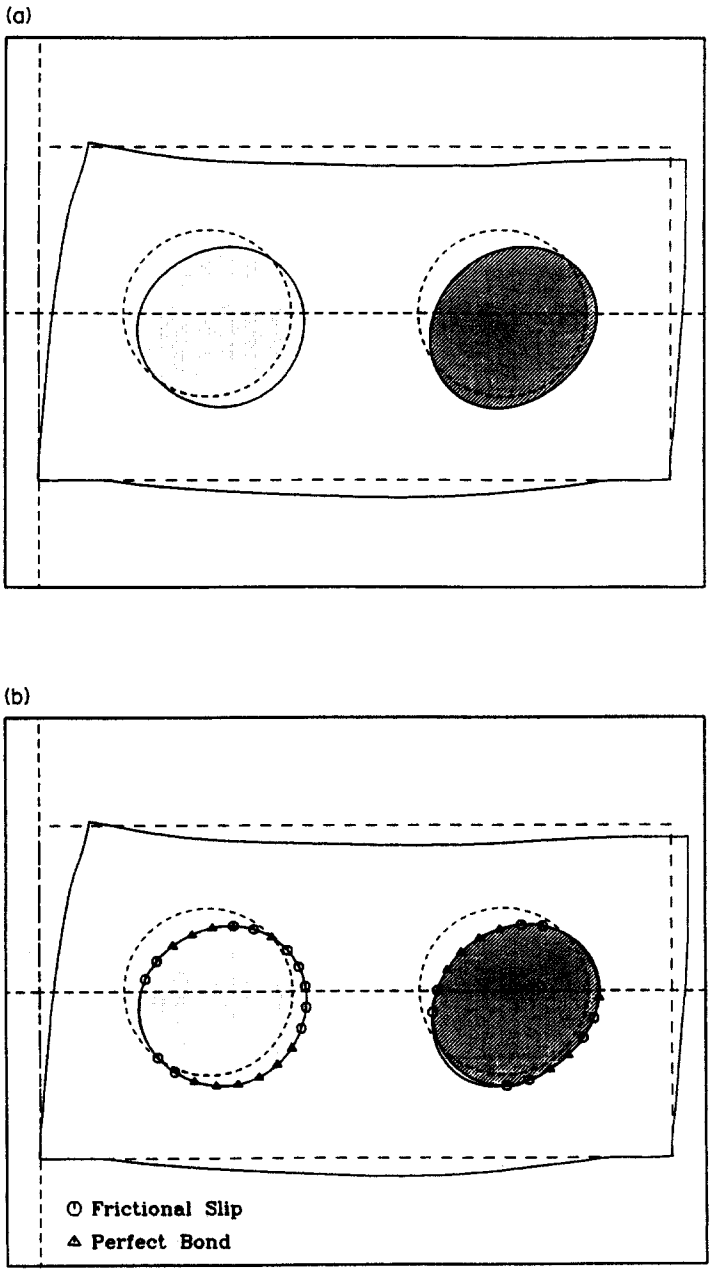

Fig. 12. Deformation pattern of composite cross-section with circular inclusions for different contact conditions. (a) Perfect bond. (b) Frictional slip ($\mu = 0.75$).

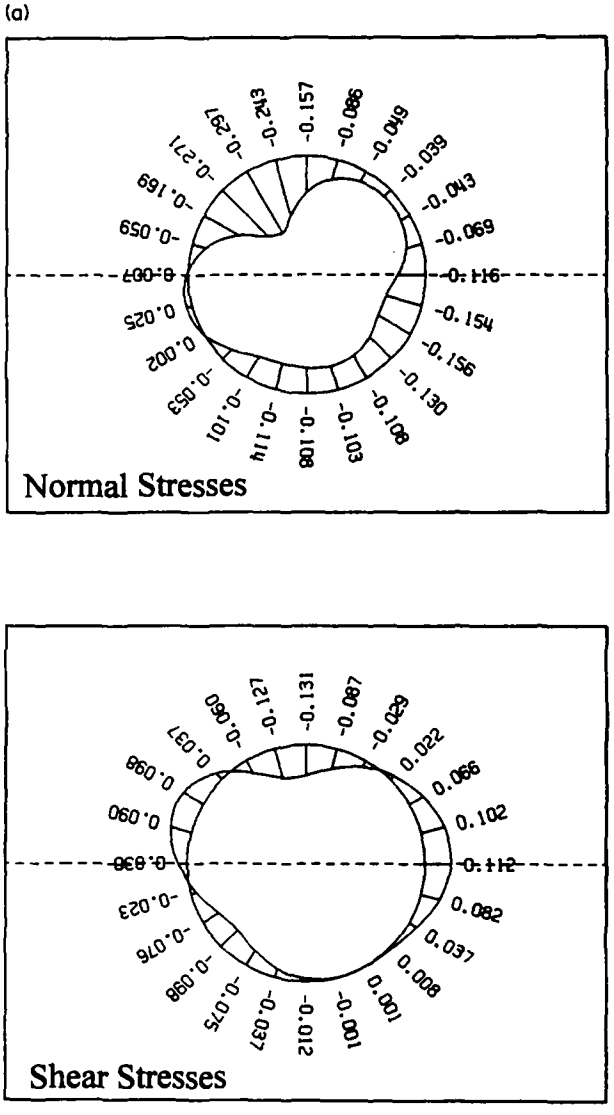

Fig. 13. Distribution of stresses developed on the matrix along the interface with inclusion No. 1 (all stresses are normalized, σ_{ij}/p). (a) Perfect bond between matrix and inclusions. (b) Frictional contact between matrix and inclusions with $\mu = 0.75$.

(b)

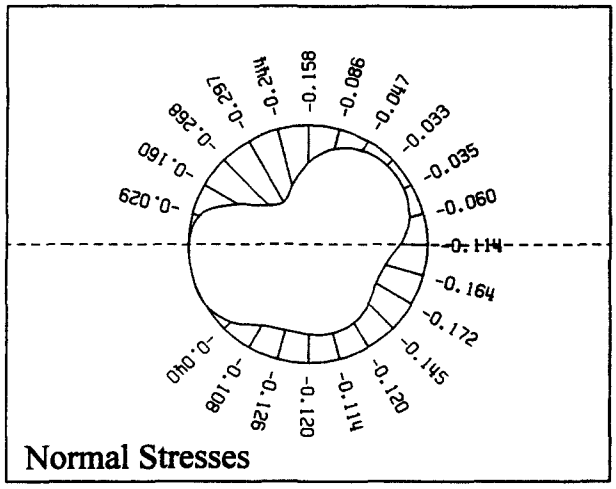

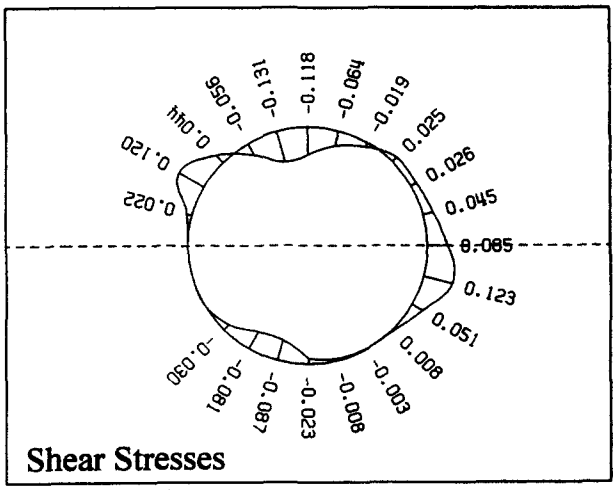

Fig. 13. *Continued.*

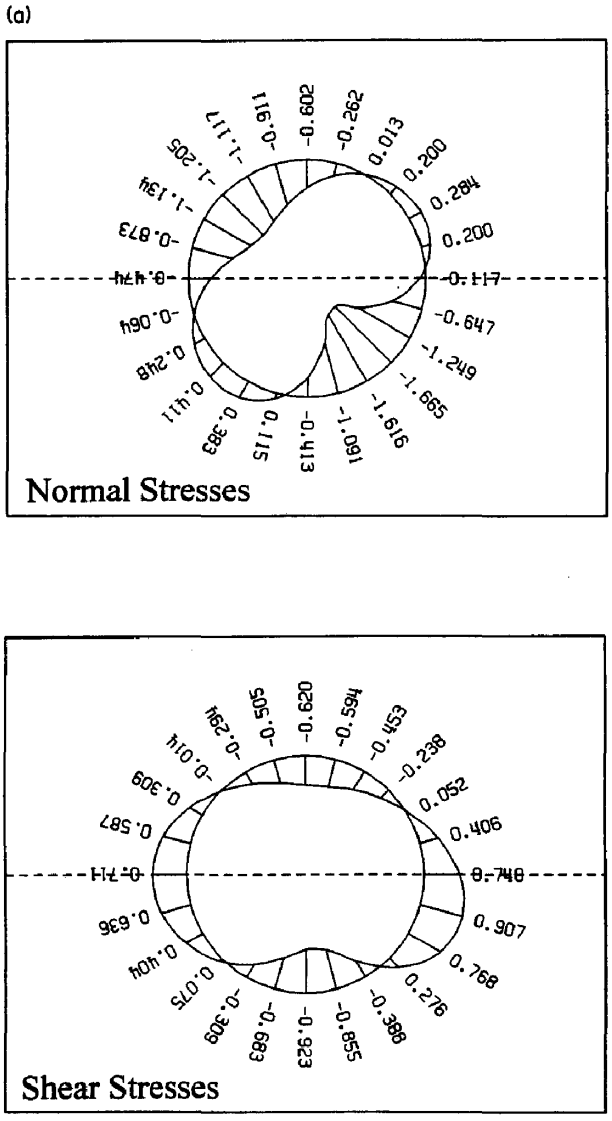

Fig. 14. Distribution of stresses developed on the matrix along the interface with inclusion No. 2 (all stresses are normalized, σ_{ij}/p). (a) Perfect bond between matrix and inclusions. (b) Frictional contact between matrix and inclusions with $\mu = 0.75$.

(b)

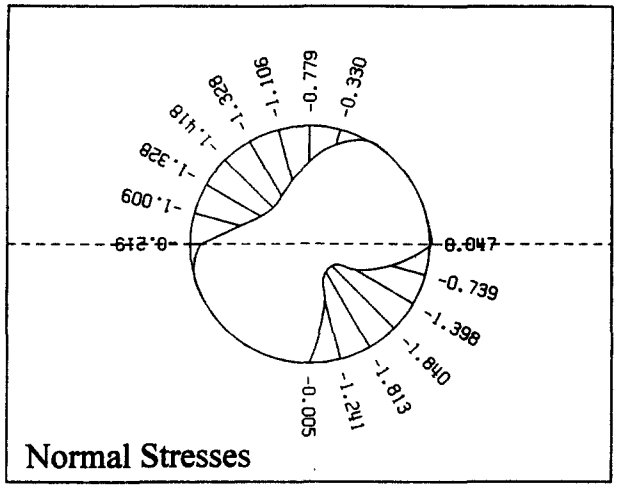

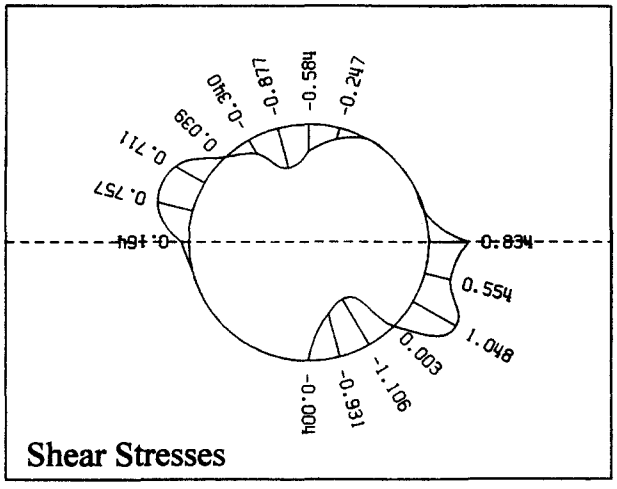

Fig. 14. *Continued.*

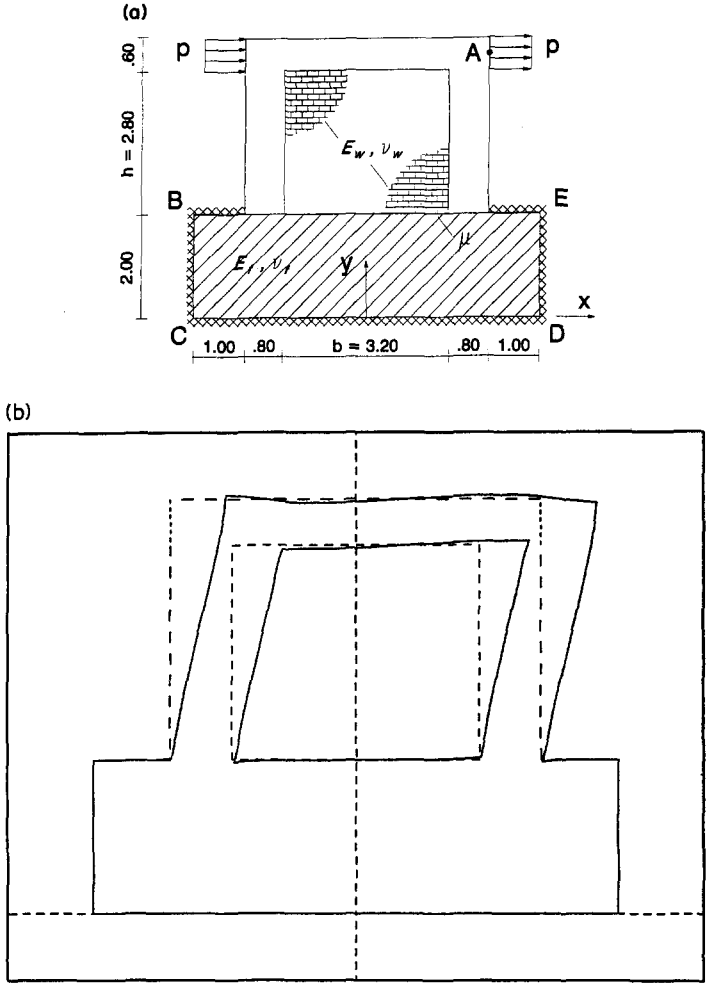

Fig. 15. Loading and deformation of a two-column frame with an infill wall of width $b = 3.20$ m and height $h = 2.80$ m. (a) Loading and support conditions. The elastic foundation has been modeled by the plane elastic body BCDE. (b) Deformed shape of the frame $E_w/E_f = 0$, $\nu_f = 0.20$ (no infill wall). (c) Deformed shape of the frame $E_w/E_f = 0.20$, $\nu_f = 0.20$, $\nu_w = 0.075$ for perfect bond along the interface. (d) Deformed shape of the frame $E_w/E_f = 0.20$, $\nu_f = 0.20$, $\nu_w = 0.075$ for frictional contact ($\mu = 0.60$) along the interface.

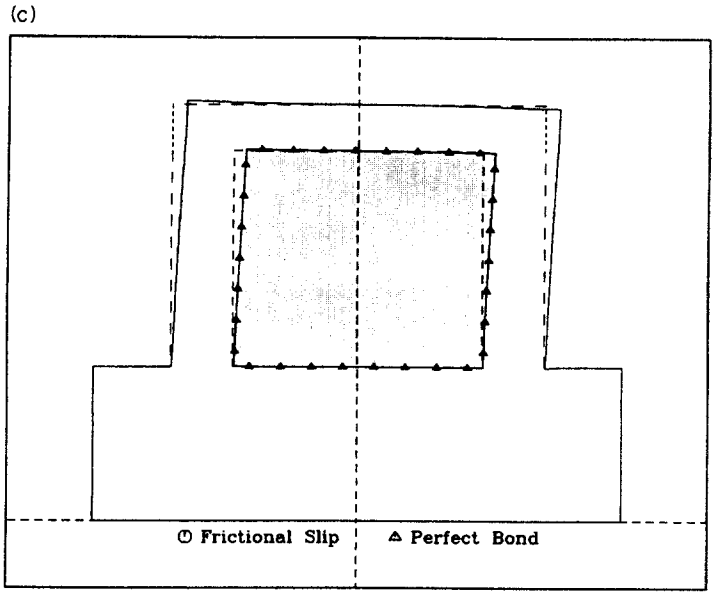

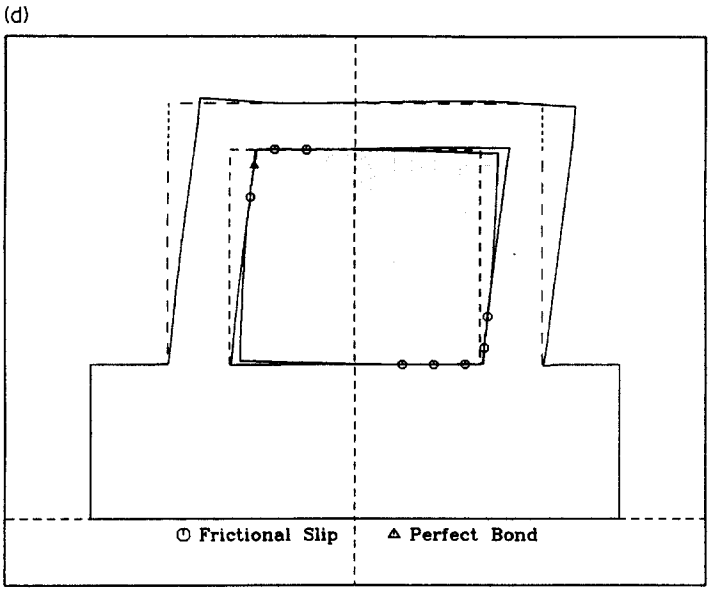

Fig. 15. *Continued.*

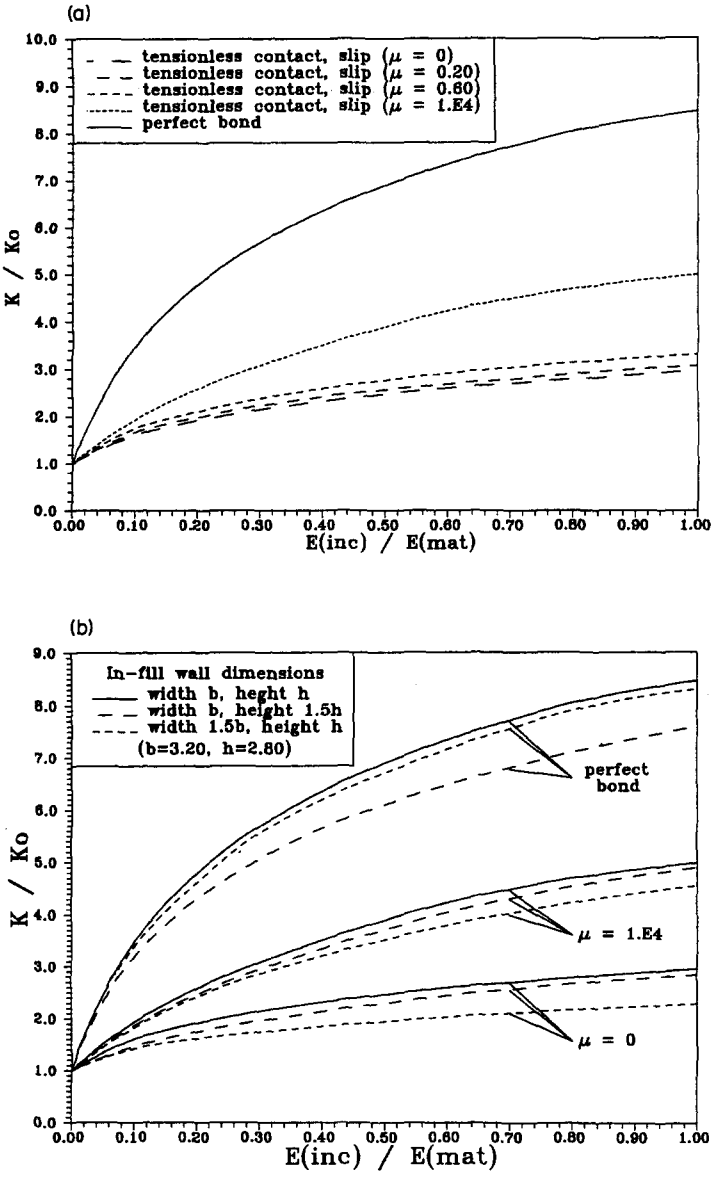

Fig. 16. Variation of the lateral stiffness K/K_0 versus the ratio of the elastic moduli of a two-column frame with an infill wall [see Fig. 15(a)], for several wall dimensions and various contact conditions. (a) Variation of K/K_0 versus E_w/E_f for a range of values of the friction coefficient μ (wall dimensions $b \times h$). K_0 is the lateral stiffness of the frame without infill wall. (b) Variation of K/K_0 versus E_w/E_f for different dimensions of the infill wall.

$P = 2 \times p \times 0.60 \times t$) versus the ratio E_w/E_f of the elastic moduli for various combinations of contact conditions. The stiffness variation is also presented graphically in Fig. 16(b) for three different ratios of the dimensions of the infill wall (h/b, $1.5h/b$ and $h/1.5b$, with $b = 3.20$ m and $h = 2.80$ m). The parametric study of Fig. 16(b) reveals that, independently of the wall dimensions, the variation of any infilled frame's lateral stiffness with respect to the ratio of the elastic moduli, will be bounded within a zone that is defined only by the friction coefficient at the interface of the two materials.

5. CONCLUDING REMARKS

An efficient boundary element approach is developed for the solution to the contact problems appearing in composite shear walls and infilled frames. The proposed method can accommodate all the variables like different material properties, complex nature of the stress system existing at the interface of the matrix and inclusions, separation, slip and loss of friction at the interface. It is an iterative technique simple in nature and converges very fast (usually four iterations are adequate). The present work is based on the total deformation formulation but can be easily extended to nonproportional loading cases by adopting an increment-type alogorithm (nonlinear analysis).

REFERENCES

Achyutha, H., Jagadish, R., Rao, P. S. and Shakeebur, R. S. (1986). Finite element simulation of the elastic behavior of infilled frames with openings. *Comput. Struct.* **23**, 685–696.

Andersson, T. (1981). The Boundary Element Method applied to two-dimensional contact problems with friction. In *Boundary Element Methods* (Edited by C. A. Brebbia), pp. 239–258. CML Publications, Springer, Berlin.

Andersson, T. (1982). The second generation boundary element contact problems. In *Boundary Element Methods in Engineering* (Edited by C. A. Brebbia), pp. 409–427. Springer, Berlin.

Andersson, T., Fredriksson, B. and Allan-Persson, B. G. (1980). The boundary element method applied to two-dimensional contact problems. In *New Developments in Boundary Element Methods* (Edited by C. A. Brebbia), pp. 247–263. CML Publications, Southampton.

Fredriksson, B. (1976). Finite Element solution of surface non-linearities in structural mechanics with special emphasis to contact and fracture mechanics problems. *Comput. Struct.* **6**, 281–290.

Gakwaya, A. and Lambert, D. (1989). A boundary element and mathematical programming approach for frictional contact problems. In *Advances in Boundary Elements* (Edited by C. A. Brebbia), Vol. 3, pp. 163–179. Springer, Berlin.

Garrido, J. A., Foces, A. and Paris, F. (1989). Three dimensional conforming frictionless contact using B.E.M. In *Advances in Boundary Elements* (Edited by C. A. Brebbia), Vol. 3, pp. 135–149. Springer, Berlin.

Heyliger, P. R. and Reddy, J. N. (1987). A mixed computational algorithm for plane contact problems—I: Formulation. *Comput. Struct.* **26**, 621–634.

Jin, H., Runesson, K. and Samuelsson, A. (1987). Application of the boundary element method to contact problems in elasticity with a nonclassical friction law. In *Boundary Elements IX* (Edited by C. A. Brebbia), Vol. 2, pp. 397–415. Springer, Berlin.

Katsikadelis, J. T. and Kokkinos, F. T. (1987). Static and dynamic analysis of composite shear walls by the boundary element method. *Acta Mech.* **68**, 231–250.

Katsikadelis, J. T. and Sapountzakis, E. J. (1985). Torsion of composite bars by the boundary element method. *J. Engng Mech. ASCE* **111**, 1197–1210.

Okamoto, N. and Nakazawa, M. (1979). Finite Element incremental contact analysis with various frictional conditions. *Int. J. Numer. Meth. Engng* **14**, 337–357.

Paris, F. and Garrido, J. A. (1985). On the use of discontinuous elements in two-dimensional contact problems. In *Boundary Elements VII* (Edited by C. A. Brebbia and G. Maier), Vol. 2, pp. 27–39. Springer, Berlin.

Paris, F. and Garrido, J. A. (1988). Friction multicontact problems with B.E.M. In *Boundary Elements X* (Edited by C. A. Brebbia), Vol. 3, pp. 305–319. Springer, Berlin.

Sachdeva, T. D. and Ramakrishnan, C. V. (1981). A finite element solution for the two-dimensional elastic contact problems with friction. *Int. J. Numer. Meth. Engng* **17**, 1257–1271.

Selvadurai, A. P. S. and Ap, M. C. (1985). Response of inclusions with interface separation, friction and slip. In *Boundary Elements VII* (Edited by C. A. Brebbia and G. Maier), Vol. 2, pp. 109–127. Springer, Berlin.

Takahashi, S. and Brebbia, C. A. (1988). Analysis of contact problems in elastic bodies using a B.E.M. flexibility approach. In *Boundary Elements X* (Edited by C. A. Brebbia), Vol. 3, pp. 353–379. Springer, Berlin.

Torstenfelt, B. (1983). Contact problems with friction in general purpose finite element computer programs. *Comput. Struct.* **16**, 487–493.

Torstenfelt, B. (1984). An automatic incrementation technique for contact problems with friction. *Comput. Struct.* **19**, 393–400.